

ChemComm

Accepted Manuscript



This is an *Accepted Manuscript*, which has been through the Royal Society of Chemistry peer review process and has been accepted for publication.

Accepted Manuscripts are published online shortly after acceptance, before technical editing, formatting and proof reading. Using this free service, authors can make their results available to the community, in citable form, before we publish the edited article. We will replace this *Accepted Manuscript* with the edited and formatted *Advance Article* as soon as it is available.

You can find more information about *Accepted Manuscripts* in the [Information for Authors](#).

Please note that technical editing may introduce minor changes to the text and/or graphics, which may alter content. The journal's standard [Terms & Conditions](#) and the [Ethical guidelines](#) still apply. In no event shall the Royal Society of Chemistry be held responsible for any errors or omissions in this *Accepted Manuscript* or any consequences arising from the use of any information it contains.

COMMUNICATION

Linkage Inversion Assembled Nano-Aptasensors (LIANAs) for Turn-On Fluorescence Detection

Cite this: DOI: 10.1039/x0xx00000x

Received 00th January 2012,
Accepted 00th January 2012Ranganathan Velu,^a Nadine Frost,^a and Maria C. DeRosa*^a

DOI: 10.1039/x0xx00000x

www.rsc.org/

A strategy for aptamer-based biosensing termed Linkage Inversion Assembled Nano-Aptasensors (LIANAs) is shown to be a generally applicable approach to the sensitive and specific detection of a target molecule in turn-on fluorescence solution-based and paper-based tests.

Aptamers are oligonucleotides that have been selected from a random library of sequences for their ability to recognize and bind a target with high affinity and specificity.¹ A multitude of biosensor platforms based on aptamers (aptasensors) have been described.² Many aptasensors rely on a conformational change in the aptamer structure to transduce the target binding event into a readable signal. As not all aptamers undergo dramatic structural changes upon target binding, a successful strategy to aptasensor development, known as structure-switching, has been described.³ Introducing a target molecule to an aptamer that has been pre-hybridized to a rationally chosen complementary sequence encodes a dramatic structural change (from duplex to complex) into the target-binding event. Based on structure-switching, the controlled assembly and disassembly of aptamer-modified nanoparticle constructs for a variety of sensor designs has been established.⁴⁻⁶ For example, the de-aggregation of pre-assembled aptamer-gold nanoparticle (AuNP) constructs has been effectively used for colorimetric detection in solution,⁷ or in lateral flow assays.⁸ Quantum dot (QD)-encoded aptamer nanostructures have been exploited for turn-on fluorescence detection of multiple targets.⁹

Aptasensor systems can be challenging to design due to a number of factors. Those relying on the dispersion of a nanoparticle assembly for detection can require the design and optimization of several unique sequences, for example different sequences for quencher (AuNP) and fluorophore (QD) labelling and a modified aptamer sequence with added complementary domains for assembly. In particular, the modified aptamer sequence could be subject to a loss of functionality with the incorporation of new domains. We

sought a system that would allow the use of the aptamer sequence without the addition of any new binding domains, and a single linker sequence that could assemble the aptamer components. The linking sequence must be long enough to ensure the formation of a reasonably stable structure with the aptamer-labelled components, but not so long that there is an increased likelihood of it folding on its own into a stable secondary structure, precluding aptasensor assembly. Here, we present a simple, generalizable approach to structure-switching aptasensors termed Linkage Inversion Assembled Nano-Aptasensors (LIANAs). (Figure 1) The assay uses a DNA linker containing a 5'-5' linkage inversion at its center (5'-5' linker) to assemble aptamer-labelled components. Linkage inversions can be introduced during oligonucleotide synthesis through the use of reversed phosphoramidites. Reversed phosphoramidites swap the positions of the dimethoxytrityl (DMT) protecting group (typically on the 5'-OH) and the phosphoramidite (typically on the 3'-OH). If these bases are used part way through a typical DNA synthesis, a 5'-5' linkage is created. We hypothesized that the use of these linkers would greatly simplify aptasensor preparation and optimization. In our system, we only employ the aptamer sequence and the short 5'-5' linker that connects the LIANA building blocks. Both the fluorophore and the quencher are functionalized with the aptamer sequence. The 5'-5' linker bridges two aptamer sequences simultaneously and the site of that bridging and the length or degree of complementarity could be altered to optimize the assay's sensitivity without having to prepare new aptamer-nanoparticle conjugates for each iteration. The presence of the linkage inversion within the linker sequence makes it less likely to adopt a stable secondary structure on its own, and allows it to bridge two aptamer sequences with less steric restrictions. Note that the linker only needs to be displaced from one of the two components of the LIANA to yield a signal and that the linker could bridge two identical sequences or two different sequences if required.

We tested this approach on the detection of Ochratoxin A (OTA). OTA is a mycotoxin produced by the genera *Aspergillus* and *Penicillium*, which grow on a variety of crops. It is found in cereals and cereal-derived products as well as other commodities including coffee, cocoa, wine, and spices.¹⁰ Considering its nephrotoxicity and potential human carcinogenicity (group 2B), inexpensive but robust methods for its detection are of critical importance. A number of OTA-specific aptamers and sensing schemes have been developed.¹¹ For the LIANAs, the aptamers known as *1.12.2*¹² and *A08min*¹³ were investigated to prepare turn-on fluorescence sensors (Figure 2). To compare this new type approach to more traditional methods for aptasensor preparation, we also tested three normal linker sequences (lacking any linkage inversion site): *10-nt*, which is the same length and composition as our 5'-5' linker, *16-nt*, and *22-nt*. Two LIANA compositions were investigated in this study. In LIANA1, AuNPs were used as quenchers for fluorescent QDs (green-emitting CdSe/ZnS). In LIANA2, gold nanorods (AuNR) were investigated as quenchers of the CdSe/ZnS QDs and red-emitting CdSeTe QDs (Figure 1). In all cases, the introduction of the 5'-5' linker DNA leads to the formation of a nanostructure complex and fluorescence quenching. Upon the addition of OTA, fluorescence is recovered due to OTA binding with its aptamer, leading to the release of the 5'-5' linker strand and disassembly of the LIANA.

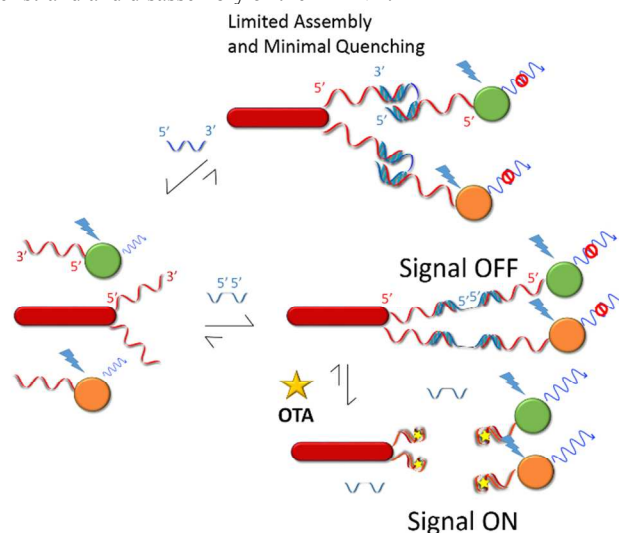


Figure 1. LIANA2: AuNRs (red rods) and QDs (green and orange circles) functionalized with OTA aptamers are assembled by a 5'-5' linker DNA and the fluorescence of the QDs is quenched. LIANA1 is assembled in a similar fashion, except with gold nanoparticles and a single type of quantum dot. When a DNA linker of the same length and composition, but lacking the inversion is used, minimal assembly is observed. OTA-induced dispersion of the nanostructures leads to a restoration of the signals.

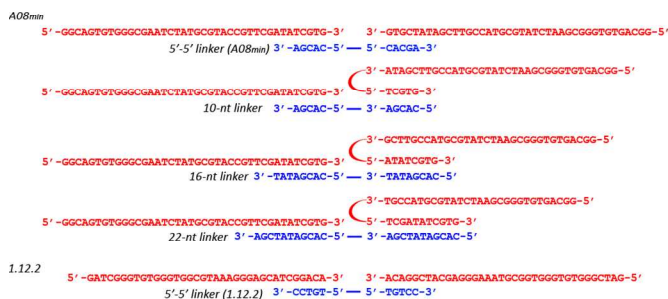


Figure 2. OTA aptamer sequences used and linkers (both 5'-5' and normal) used for assembly of the nanosensors.

For LIANA1, aptamer-AuNPs and aptamer-QDs were incubated in the absence and presence of the 5'-5' linker DNA (Figure 3). Without the linker, the aptamer-AuNPs and aptamer-QDs were seen to be well-dispersed and aggregate-free using TEM. In the presence of the linker, a halo of quantum dots could be observed surrounding the gold nanoparticles. After incubation with OTA (30 min.), the AuNPs and QDs were once again observed to be well-dispersed, providing support for the proposed LIANA1 assembly mechanism and target-induced disassembly. Similar observations were noted with LIANA2 (Figure 3 d-f). Confocal laser scanning microscopy (CLSM) confirmed the fluorescence properties of the LIANAs upon assembly/disassembly (Figure S1). A physical mixture of the aptamer-labeled QDs and AuNPs or AuNRs did not lead to QD quenching (Figure S1) while addition of 5'-5' linker to the mixture initiates assembly and results in a clear quenching of the QD fluorescence. Fluorescence recovery is noted within 30 minutes of OTA addition, confirming the re-dispersion of the components. We attempted to assemble the nanomaterial components using linkers lacking the 5'-5' inversion (see Figure 3g-i) and saw little to no evidence of assembly. No assemblies could be found with *10-nt*, the linker of identical length and composition to the 5'-5' linker. Using the 5'-5' inversion may eliminate some steric restrictions allowing for a much shorter linker to be used. Even with longer linkers, such as *16-nt* and *22-nt*, only minimal assembly of the nanomaterials could be observed. Notably, *22-nt* showed only sporadic evidence of assembly (<5% of AuNRs imaged showed evidence of any interaction with QDs, see Fig3I), despite its long length. Melting temperature analysis (T_m) by variable temperature UV-Vis spectroscopy indicated that *22-nt* on its own showed a high degree of secondary structure (Figure S2) which may preclude it from interacting with the aptamer-modified components. Undoubtedly, with extensive trial and error, a usable extended linker sequence lacking the 5'-5' inversion could be designed; these observations confirm, however, that the 5'-5' linker approach can help to simplify aptasensor design. Also note that QD-QD and/or AuNR-AuNR or AuNP-AuNP assemblies are also possible given this approach. (See Figure S3). Interestingly, these were seen only rarely and can be mitigated by thorough mixing of the aptamer-modified component prior to linker addition.

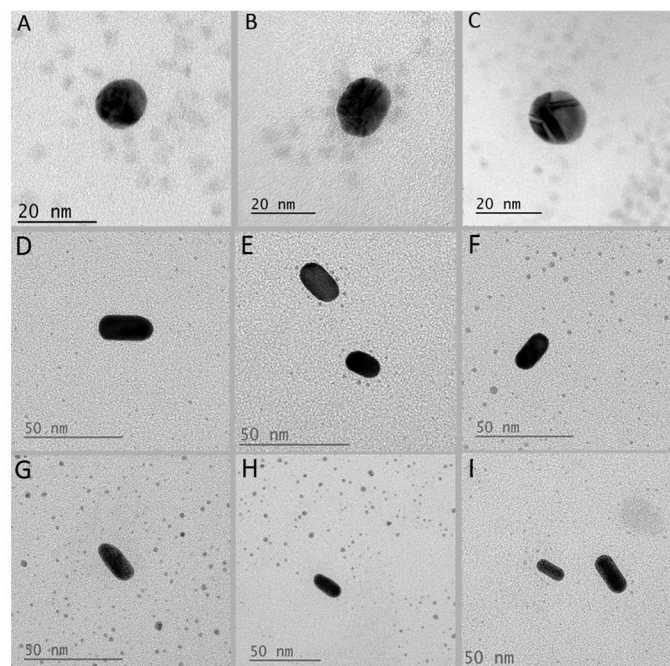


Figure 3. (a-c) LIANAs from *1.12.2* OTA aptamer were used for these images a) TEM image of aptamer-modified AuNPs and QDs prior to incubation with the 5'-5' linker. b) LIANA1 showing QDs closely associating with the gold nanoparticle. c) LIANA1 after the addition of 1.8 μM of OTA, causing dispersion of the nanoparticles. (d-f) LIANAs from *A08* aptamer were used for these images. d) TEM image of aptamer-modified AuNRs and QDs in the absence of linker. e) LIANA2 after addition of linker DNA. f) After the addition of OTA (1.8 μM), LIANA2 disassembles into free QDs and AuNRs. (g-i) Attempts to make assemblies using normal (no 5'-5' inversion) linkers shows minimal to no assembly. g) Aptamer-modified AuNRs and QDs in the presence of 10-nt linker (0.1 μM). h) Aptamer-modified AuNRs and QDs in presence of 16-nt linker (0.1 μM). i) Aptamer-modified AuNRs and QDs in the presence of 22-nt linker (0.1 μM).

With the feasibility of the approach confirmed, solution- and paper-based biosensors were investigated. The photoluminescence (PL) spectra from the two LIANA systems are shown in Figure 4. Assembly of LIANA1 can be monitored by PL quenching (Figure 4a). When LIANA1 is exposed to increasing concentrations of OTA, an increase in QD fluorescence can be observed (Figure 4b). Plotting the normalized PL intensity vs. OTA concentration (Inset Figure 4b) reveals a concentration-dependent increase in QD signal (LOD of 130 nM, linear range to 1.5 μM), while no effect is noted from addition of OTA to aptamer-QDs alone (Figure S4) nor for structurally-related targets Ochratoxin B (OTB) or warfarin (Inset Figure 4b). LIANA2 has the added advantage that AuNRs display two surface plasmon resonance bands that overlap well with the emission of two different types of QDs (green and red emitters). LIANAs comprised of both QD types labelled with the same aptamer (either *1.12.2* or *A08*). Assembly in the presence of the linker and disassembly with OTA (Figure 4C and D) could be tracked by changes in fluorescence. Plotting normalized PL intensity vs. concentration at each of the two wavelengths (Inset Figure 4 D) confirmed that both signals could be used for OTA detection (LOD of 130 and 200 nM, respectively). Once again, the lack of PL quenching observed with the use of standard linkers of increasing lengths confirmed the effectiveness of the LIANA approach. (Figure S5) Furthermore, the specificity for OTA was retained in the LIANA system, with no response noted from structurally related compounds OTB and warfarin (Figure S7 and Inset Figure 4D). To ensure the generality of the approach, mixed LIANA2 samples were prepared using both OTA aptamers (*1.12.2* and *A08min*) (Figure S6). *A08min*-modified QDs (red) and *1.12.2*-modified QDs (green) were linked to AuNRs using their respective 5'-5' linkers. Despite differences in the sequences and structures of these two aptamers, OTA concentration-dependent increases in the signals from both QDs could be detected, with slightly different sensitivities as imposed by aptamer affinity. This suggests that our approach is general and independent of aptamer structure. Multiple aptamers for the same target could be used in the LIANAs to further validate target detection, or to extend the linear dynamic range of the system. Alternatively, aptamers for different targets could be explored for multiplexed detection. Additionally, the efficacy of the solution-based sensor in the presence of real samples was examined using OTA-spiked complex extracts (Figure 5A). OTA-dependent regeneration of the QD fluorescence was noted to about 50% of the original signal prior to LIANA2 assembly, likely due to the quenching effects of other matrix components. Nevertheless, the

LIANA approach was deemed feasible for target detection in both simple and complex matrices.

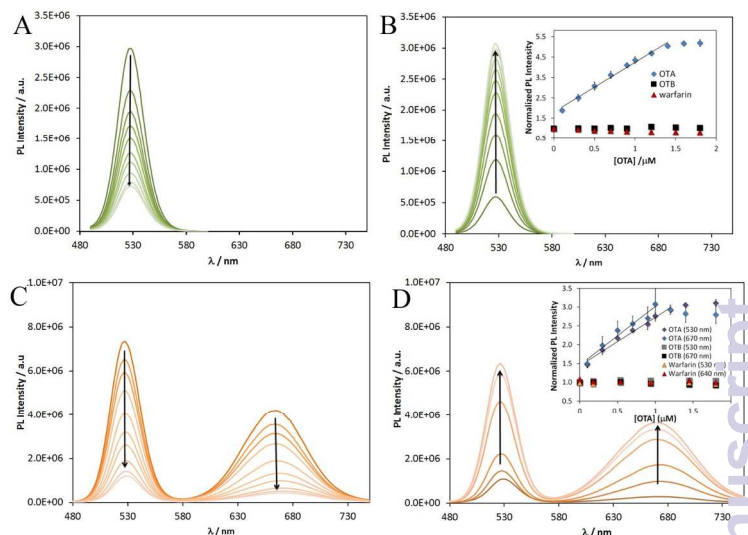


Figure 4. a) LIANA1 assembly with increasing 5'-5' linker (0-0.1 μM). b) PL signal of LIANA1 with increasing OTA (0, 0.18, 0.36, 0.56, 0.7, 0.9, 1.0, 1.2, 1.45, 1.63, and 1.8 μM) in buffer A solution inset: Normalized PL intensity versus OTA concentration added to LIANA1, illustrating the sensitivity, linear dynamic range, as well as selectivity for OTA over OTB and warfarin. ($y = 2.445x + 1.7965$, $R^2 = 0.9888$) c) PL changes of LIANA2 during assembly (0-0.1 μM 5'-5' linker). d) PL with increasing OTA (0, 0.18, 0.54, 0.94, 1.45 and 1.8 μM) in buffer B solution. Inset: Relative PL at 530 nm ($y = 1.2902x + 1.4375$, $R^2 = 0.9827$) and 670 nm ($y = 1.5646x + 1.4537$, $R^2 = 0.957$) versus OTA concentration, illustrating the sensitivity and linear dynamic range, as well selectivity for OTA over OTB and warfarin. *1.12.2* aptamer was used for LIANA1 and *A08min* was used for LIANA2.

Lastly, we applied the LIANA approach to a simple, rapid, paper-based detection system. Paper assays are gaining widespread attention in diagnostic sciences because of their low cost and ease of use. DNA-nanoparticle paper-based assays have been developed for the detection of nucleic acid and non-nucleic-acid targets.¹⁴⁻¹⁶ LIANA2 samples were spotted on unmodified filter paper. OTA-spiked complex extract (mixed wheat, barley, corn, oats, and malted barley) was spotted onto the LIANA zones of the paper and compared to control zones of either the OTA-free complex extract on LIANA zones, or OTA alone (Figure 4). Visual detection of OTA down to 10 nM could be achieved using a simple hand-held UV-light and camera, without paper functionalization or the need for advanced equipment. The improved LOD compared to the in-solution assay could be attributed to a pre-concentration effect of the paper matrix. Our paper-based detection system is comparable in terms of the LOD for visual detection of OTA in a complex matrix with another fluorescence dipstick assay (12 nM LOD).¹⁷

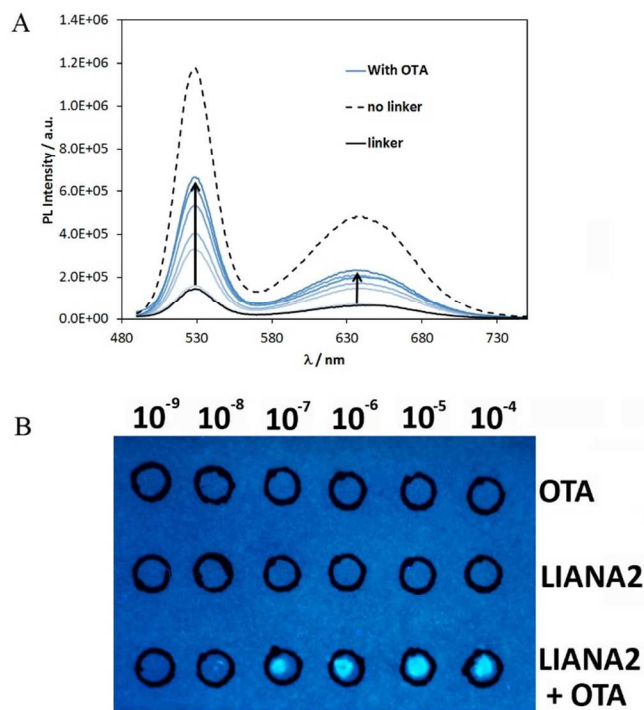


Figure 5. a) LIANA2 system with OTA-spiked complex solutions. After assembly of the LIANA (black line), OTA-induced disassembly leads to an increase in the fluorescence signals (blue lines), to 50% of the original signal prior to assembly (dashed line). The loss of fluorescence in comparison to buffer solution is attributed to matrix effects. b) Paper-based LIANA: LIANA2 samples (1 μ L) were spotted into the bottom two rows of black circles. Top: 1 μ L OTA from 10^{-4} to 10^{-9} M spiked into complex extract as a control. Middle: 1 μ L of complex extract spotted onto each of the LIANA2 zones. Bottom: 1 μ L OTA from 10^{-4} to 10^{-9} M spiked into complex extract and spotted on the LIANA2 zones. $A08_{min}$ aptamer was used for these images.

In conclusion, these studies confirm the feasibility of the LIANA approach to biosensor development. The use of the short linker containing a 5'-5' linkage inversion to bridge aptamer-modified components is simple, cost-effective, and generally applicable. The LIANAs ensure a significant structural change occurs upon target binding that can be transduced into a signal change with excellent sensitivity and selectivity. The LIANA approach was applied to fluorescence-based OTA detection, and was found to be effective in solution and paper-based assays, even in a complex matrix. Future work will establish how LIANAs can be applied to other biosensor platforms (e.g. colorimetric, etc.) for the detection of important targets in a variety of complex matrices.

Notes and references

^a R. Velu, N. Frost, M. C. Derosa*

Department of Chemistry

Carleton University

1125 Colonel By Drive, Ottawa, ON, Canada, K1S 5B6

E-mail: maria.derosa@carleton.ca

Electronic Supplementary Information (ESI) available: experimental procedures, CLSM images, fluorescence data from control experiments. See DOI: 10.1039/c000000x/

1 G. Mayer, *Angew. Chem. Int. Ed.*, 2009, **48**, 2672-89.

2. E.J. Cho, J. Lee, A.D. Ellington, *Annu Rev Anal Chem*, 2009, **2**, 241-64.
3. R. Nutiu, Y. Li, *J Am Chem Soc*, 2003, **125**, 4771-8.
4. R. Kong, X. Zhang, Z. Chen, W. Tan, *Small*, 2011, **7**, 2428-36.
5. J. Li, X. Zhong, H. Zhang, X. C. Le, J.-J. Zhu *Anal. Chem* 2012, **84**, 5170-5174.
6. Z. Zhou, Y. Du, S. Dong, *Biosens. Bioelect.* 2011, **28**, 33-37.
7. J. Liu, Y. Lu, *Angew. Chem. Int. Ed.*, 2006, **45**, 90-94.
8. J. Liu, D. Mazumdari, Y. Lu, *Angew. Chem. Int. Ed.*, 2006, **45**, 7955-59.
9. J. Liu, J.H. Lee, Y. Li, *Anal Chem*, 2007, **79**, 4120-25.
10. A.E. Khoury, A. Atoui, *Toxins*, 2010, **2**, 461-93.
11. A. Rhouati, C. Yang, A. Hayat, J.L. Marty, *Toxins*, 2013, **5**, 1988-2008.
12. J.A. Cruz-Aguado, G. Penner, *J Agric Food Chem*, 2008, **56**, 10456-61.
13. M. McKeague, R. Velu, K. Hill, V. Bardoczy, T. Meszaros, M.C. DeRosa, *Toxins*, 2014, **6**, 2435-52.
14. M.O. Noor, A. Shahmuradyan, U.J. Krull, *Anal Chem*, 2013, **85**, 1860-67.
15. W. Zhao, M.M. Ali, S.D. Aguirre, M.A. Brook, Y. Li, *Anal Chem*, 2008, **80**, 8431-37.
16. M. He, Z. Liu, *Anal Chem*, 2013, **85**, 11691-94.
17. L. Wang, W. Chen, W. Ma, L. Liu, W. Ma, Y. Zhao, W. Zhu, L. Xu, H. Kuang, C. Xu, *Chem. Commun.* 2011, **47**, 1574-1576.